Phase transitions in dissipative Josephson chains: Monte Carlo results and response functions

P. A. Bobbert, Rosario Fazio,* and Gerd Schön
Department of Applied Physics, Delft University of Technology, Lorentweg 1, 2628 CJ Delft, The Netherlands

A. D. Zaikin
Department of Theoretical Physics, Lebedev Physics Institute, Moscow, U.S.S.R.
(Received 20 February 1991; revised manuscript received 1 July 1991)

A chain of Josephson junctions shunted by Ohmic resistors undergoes phase transitions at zero temperature that result from the interplay between quantum fluctuations induced by charging effects and the dissipation. The quantum-mechanical partition function expressed in terms of phase slips in space-time can be mapped onto that of a two-dimensional Coulomb gas. Due to the dissipation the interaction is anisotropic. Despite the simplicity of the model, there is no general agreement about the phase diagram and the response functions. We have performed Monte Carlo simulations to determine the zero-temperature phase boundaries. We find four phases with the absence or presence of global or local order, in all combinations. We discuss the response functions in the different phases and find interesting transport properties.

I. INTRODUCTION AND SUMMARY

Experiments on two-dimensional (2D) superconducting granular films[1] and lithographically manufactured arrays of Josephson junctions[2] have initiated substantial theoretical effort to investigate the low-temperature properties of dissipative junction arrays. The interplay between quantum fluctuations, induced by charging effects, and the dissipation in these systems can lead to rich phase diagrams. The dissipation may be due to quasiparticle tunneling or to ohmic shunts.[3,4] Arrays with both types of dissipation have been studied by various techniques,[5-14] although, because of its simplicity, the majority of the theoretical papers concentrated on ohmic dissipation. The strength of the ohmic dissipation is characterized by the ratio $\alpha = R_Q/R_S$ of the quantum resistance $R_Q = h/4e^2 = 6.45$ kΩ and shunt resistance R_S. Regular arrays of Josephson junctions, depending on the dimensionality and temperature, undergo phase transitions to long-range order or a Kosterlitz-Thouless-Berezinkii (KTB) transition. But in addition, because of the dissipation, there exists a $T=0$ transition to *local* order.[8,9] The critical strength of the dissipation is $\alpha = 1/z$ or $2/z$, in the limit of large or small ratios of the Josephson energy E_J and scale of the charging energy E_C, respectively. Here z is the coordination number of the lattice.

The $T=0$ transitions can also be studied in a linear chain of Josephson junctions.[10-12] If the charging energy is due to the nearest-neighbor capacitance only, the junctions effectively decouple,[5(c)] and one is left with the single-junction problem discussed in Ref. 15. More interesting is the case where the charging energy arises as a result of a self-capacitance (capacitance to infinity or ground) or where both capacitances matter.[11] With the Villain transformation[10,12] or by instanton techniques[11]—both require not too small values of the ratio E_J/E_C—the quantum-mechanical partition function of the chain of Josephson junctions can be mapped onto that of a 2D Coulomb gas in space- (imaginary) time. The phase slips of the phase difference of the superconducting order parameters across the junctions correspond to the charges of the Coulomb gas. In the limit of vanishing dissipation, the charges have an isotropic logarithmic interaction in space-time.[16] As a result, a KTB transition occurs from a disordered to a dipole phase at a critical value of the ratio between E_J and E_C. The dissipation caused by an ohmic shunt gives rise to an additional, strongly anisotropic interaction between the charges in time direction. This induces further phase transitions. For small Josephson energy at $T=0$, a phase transition occurs at $\alpha=1$ between a disordered phase ($\alpha<1$) and a phase with local, but no global order ($\alpha>1$).[10] For large Josephson energy a phase transition occurs at $\alpha=\frac{1}{2}$.[11,12] In a previous publication[12] we identified the last transition as a transition between a dipole and a *quadrupole* phase, since in the latter the charges in space-time are arranged in quadrupoles.

The phase diagrams obtained in Refs. 10–12 differ in important aspects. Also, the transport properties of the different phases are still debated. Panyukov and Zaikin[9,13] claimed that only the phase with large Josephson energy and strong dissipation can be called superconducting. This is in conflict with the results of Bradley and Doniach[16] and Zwerger,[10] who found a phase transition to a superconducting state for zero or weak dissipation. Another interesting claim was made by Zwerger:[10] He states that the phase with only local order, i.e., for small Josephson energy and $\alpha>1$, has a vanishing resistance, but no Meissner effect.

It is the purpose of this paper to resolve the remaining questions about the zero-temperature phase diagram and the transport properties of the different phases. We consider a chain of Josephson junctions with self-capacitance only, which are shunted by ohmic resistors. In Sec. II we

define the model and the mapping of its partition function onto that of a 2D Coulomb gas in space-time. The analytical predictions for the phase diagram are reviewed in Sec. III. In order to check these predictions, we performed Monte Carlo simulations of this Coulomb gas, which we present in Sec. IV. In Sec. V we discuss the response functions in all phases.

To set the stage and label the different phases, we display the phase diagram following from our simulations in Fig. 1. We find conclusive evidence for four different phases.

(I) For small Josephson energy (as compared to the charging energy) and weak dissipation, the chain is in a *disordered* or *plasma phase,* with an infinite dielectric constant.

(II) For large Josephson energy and weak dissipation, the chain is in a *dipole* or *dielectric phase.* This phase is characterized by global order and a finite dielectric constant. Locally, however, there remains some disorder, which is expressed by the fact that the phase difference at each junction changes as a function of time.

(III) For large Josephson energy and strong dissipation, the chain is in a *quadrupole phase,* again characterized by global order and a finite dielectric constant. But in this phase there exists also local order: The phase difference at each junction remains localized in time. We will see that we can distinguish another crossover within this phase, dividing it further into regions (IIIa) and (IIIb) with different response functions.

(IV) For small Josephson energy and strong dissipation, the chain is in a phase with only *local order.* The phase difference at each junction is localized, but there exists no global order and the dielectric constant is infinite.

Our main conclusions concerning the response functions are listed in Table I. We determine the transport properties of the system in two different experimental configurations. The first is a chain forming a ring of circumference N_x (approaching infinity) which encloses a time-dependent flux. We calculate the average current in the chain and, from that, the conductance. The second configuration is an infinite chain with a current imposed to flow through a finite part of length L_x of the chain. We calculate the average voltage across this finite part and, from that, an impedance. This configuration was suggested in Ref. 13. In both configurations we distinguish vanishing $\omega \ll 1/N_x, 1/L_x$ and finite frequencies

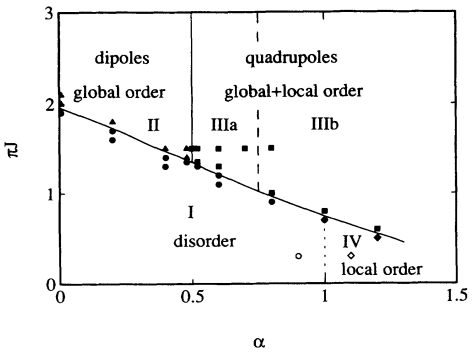

FIG. 1. Phase diagram of the resistively shunted chain of Josephson junctions with self-capacitance, following from the Monte Carlo simulations for the anisotropic Coulomb gas of its phase slips in space-time. The strength of the dissipation is characterized by the ratio $\alpha = R_Q/R_S$, with R_Q the quantum resistance and R_S the shunt resistance. The parameter $J = \sqrt{E_J/8E_C}$ controls the strength of the quantum fluctuations, with E_J the Josephson energy and $E_C = e^2/2C$ the scale of the charging energy. The simulations indicated by the open symbols were obtained with an artificial reduction of the activity of the phase slips, and the dotted line is the theoretical prediction for the phase transition for small J. The dashed line represents the crossover in the self-energy found to fourth order in the activity of the phase slips. "Global order" is to be understood in the KTB sense (algebraic decay of correlation functions).

$1/N_x, 1/L_x \ll \omega \ll 1$, where the frequency ω is scaled in units of the Josephson plasma frequency.

For the case $1/N_x \ll \omega \ll 1$ in the first configuration, we encounter three different results. In the disordered phase (I), the conductance equals that of a classical RC chain, with $R = R_S$ and C the capacitance to ground; the Josephson channel is blocked. In the dipole (II) and quadrupole (III) phases, the Josephson channel is opened, and the conductance equals that of a classical LC chain with $L = \delta/4e^2E_J$. Here E_J is the Josephson energy and δ (≥ 1) a constant depending on the exact location in the phase diagram. In the phase (IV) with only local order, we find a nontrivial frequency dependence of the conductance which is neither that of an RC nor that of an LC chain. For the case $\omega \ll 1/N_x$, we find infinite conductance in phases (II), (III), and (IV) and a finite conductance equal to $1/N_x R_S$ in phase (I). The infinite conductance in phases (II) and (III) is associated with a finite

TABLE I. Response functions in the different phases and for the two different configurations (see the text). By JC chain we mean the response of a chain with the Josephson channel opened. We distinguish two frequency ranges $1/N_x, L_x \ll \omega \ll 1$ or $\omega \ll 1/N_x, L_x$. From the latter results we determine whether a finite superfluid density n_s is present. The asterisk in the last column indicates that this result was obtained in an indirect way (see the text).

	Configuration 1: flux through ring (length N_s)			Configuration 2: open section (length L_x)		
Phase	$1/N_x << \omega << 1$	$\omega << 1/N_x$	n_s	$1/L_x << \omega << 1$	$\omega << 1/L_x$	n_s
(I)	$R_S C$ chain	$\sigma = 1/N_x R_S$	0	$R_S C$ chain	$Z = L_x R_S$	
(II)				RC chain ($R < R_S$)		0
(IIIa)	JC chain	$\sigma = \infty$	finite	JC chain		
(IIIb)					$Z = 0$	finite
(IV)	anomalous		0	anomalous		0

superfluid density n_s. However, in phase (IV), the phase with only local order, the superfluid density vanishes. A comment on semantics: A chain of junctions cannot expell a magnetic field. Hence, strictly speaking, there exists no Meissner effect. Nevertheless, a finite or vanishing superfluid density has been denoted as presence or absence of a "Meissner effect."[10]

The results for the impedance in the second configuration for finite frequencies, $1/L_x \ll \omega \ll 1$, agree with the results in the first configuration (impedance equals the inverse of the conductance) with one exception: In the dipole phase (II), the impedance is that of an RC chain, but with $R < R_S$. In the case $\omega \ll 1/L_x$, we now find resistive behavior in the disordered (I) and dipole (II) phases, with $R = L_x R_S$. In the quadrupole (III) and locally ordered phase (IV), the resistance vanishes. If, following Ref. 13, we invert the impedance obtained in the second configuration to get the conductance and then infer the superfluid density by multiplying this conductance with ω, we find that this "superfluid density" is finite only in region (IIIb). We have to stress, however, that this result contradicts the result obtained in the direct determination of n_s in the first configuration.

We see that the response functions differ in the two configurations. This explains the apparent disagreement between the results of Zwerger[10] and those of Panyukov and Zaikin.[9,13] Comparing the phase diagram with those of Refs. 10–13, we find further qualitative and quantitative differences. An elaborate discussion will follow in Sec. V.

II. MODEL

We study a chain of superconducting islands with Josephson coupling energy E_J and with self-capacitance (capacitance to ground) C, leading to a charging energy scale $E_C = e^2/2C$. The dissipation is caused by a shunt resistance R_S across each junction. The action of this system reads (we put $\hbar = 1$)

$$A[\varphi] = \sum_i \left\{ \int_0^\beta d\tau \left[\frac{1}{16E_C} \left(\frac{d\varphi_i}{d\tau} \right)^2 - E_J \cos \nabla_x \varphi_i(\tau) \right] + \frac{1}{2} \int_0^\beta d\tau \int_0^\beta d\tau' \, \alpha(\tau - \tau') \times [\nabla_x \varphi_i(\tau) - \nabla_x \varphi_i(\tau')]^2 \right\} , \quad (1)$$

where $\varphi_i(\tau)$ is the phase of the superconducting order parameter in the island i at (imaginary) time τ, β is the inverse temperature, and $\nabla_x \varphi_i(\tau) = \varphi_{i+1}(\tau) - \varphi_i(\tau)$ is the lattice derivative. The Fourier transform of the dissipative kernel is

$$\alpha(\omega) = -\frac{\alpha}{4\pi} |\omega| , \quad \alpha = \frac{R_Q}{R_S} , \quad (2)$$

with $R_Q = h/4e^2$ the quantum of resistance. The associated partition function can be expressed as a path integral

$$Z = \int \prod_i D\varphi_i(\tau) \exp(-A[\varphi]) . \quad (3)$$

The variables $\varphi_i(\tau)$ are defined on the interval $[-\infty, \infty]$ and satisfy the boundary conditions $\varphi_i(\beta) = \varphi_i(0)$, pertaining to systems with ohmic dissipation, where the charges can take any continuous value, and states with phases differing by multiples of 2π are distinguishable.[17]

A small E_J expansion in the integral in (3) yields a description in terms of a gas of positive and negative "charges" at each junction, which represent Cooper pair tunneling events. For large separations in space-time between these charges, their interaction becomes diagonal in the junction number and logarithmic in time, with strength proportional to $2/\alpha$. This implies that, at zero temperature, a phase transition occurs at $\alpha = 1$, between a phase where Cooper pairs are delocalized ($\alpha > 1$) to a phase where they are localized ($\alpha < 1$).[8,9,12]

Further transitions are found in the limit of large and moderate values of E_J. In this case the action (3) can be made tractable by using the Villain transformation for the Josephson term.[10,12] For this the time is discretized in slices $\Delta\tau$, and at each space-time lattice point (dual lattice points in space) an integer valued field $n(j,\tau)$ is introduced with the result that the action becomes quadratic in φ. Here j denotes the junction j between islands j and $j+1$, and for simplicity we continue to use τ to denote the discrete times. The natural choice for the time slices is $\Delta\tau = 1/\sqrt{8E_J E_C}$, which leads to a symmetric description in space-time in the absence of dissipation.[16] In Fourier language the partition function now assumes the form

$$Z = \sum_{\{n\}} \int D\varphi(k,\omega) \exp\left[-\frac{J}{2N} \sum_{k,\omega} [2(1-\cos\omega) + \lambda|\omega|2(1-\cos k)] |\varphi(k,\omega)|^2 + |[1-\exp(ik)]\varphi(k,\omega) - 2\pi n(k,\omega)|^2 \right] . \quad (4)$$

Here we define the reduced coupling constants

$$J \equiv \sqrt{E_J/8E_C} , \quad \lambda \equiv \alpha/(2\pi J) , \quad (5)$$

and we have scaled the frequency ω in units of the Josephson plasma frequency $\sqrt{8E_J E_C}$. The sum in the action of (4) is over wave vectors k and frequencies ω from the first Brillouin zone $|k|, |\omega| \le \pi$. Both are integer multiples of $2\pi/N_x$ and $2\pi/N_\tau$, where N_x is the number of islands and N_τ the number of time slices, respectively, and $N = N_x N_\tau$. We have taken periodic

boundary conditions in space: $\varphi_{i=0}=\varphi_{i=N_x}$. The integration over the phases φ in (4) is straightforward and yields a spin-wave contribution $Z_{\rm SW}$. The partition function can now be expressed in terms of the integer field $n(j,\tau)$ only. For this it is convenient to introduce a new integer field $p(j,\tau)$ by

$$p(j,\tau)\equiv\nabla_\tau n(j,\tau)=n(j,\tau+\Delta\tau)-n(j,\tau)\ , \tag{6}$$

which represents the "phase slips" at junction j. Hence

$$Z=Z_{\rm SW}\sum_{\{p\}}\exp\left[-\frac{2\pi^2}{N}\sum_{k,\omega}|p(k,\omega)|^2G_0(k,\omega)\right]\ . \tag{7}$$

The Green function $G_0(k,\omega)$ in this expression is given by

$$G_0(k,\omega)=\frac{J}{\omega^2}\,\frac{\omega^2+\lambda k^2|\omega|}{k^2+\lambda k^2|\omega|+\omega^2}\ , \tag{8}$$

in which we write for short k^2 and ω^2 for $2(1-\cos k)$ and $2(1-\cos\omega)$. Also, $|\omega|$ is understood to be periodic. The details at the boundary of the Brillouin zone, which depend on the choice of the time cutoff $\Delta\tau$, do not matter in the following. For large enough distances in space-time, the interaction (8) can be approximated by

$$G_0(k,\omega)\approx\frac{J}{k^2+\omega^2}+\frac{\alpha|\omega|}{2\pi\omega^2}=G_0^I(k,\omega)+G_0^A(k,\omega)\ . \tag{9}$$

The partition function (7) describes a Coulomb gas of integer charges, which for the large distances in space-time have an isotropic logarithmic interaction, with prefactor $2\pi J$, and a strongly anisotropic logarithmic interaction in the time direction (between charges at the same junction), with prefactor 2α. The pole of the propagator (8) at $k=\omega=0$ implies overall charge neutrality. The pole at $\omega=0$ implies charge neutrality in time of the phase slips at each junction. In principle, the integer field $p(j,\tau)$ can take all integer values, but we can restrict ourselves to $p=0,\pm1$, since higher values are exponentially suppressed.

The derivation by means of the Villain transformation, used here, can easily be reformulated in terms of the instanton picture used by Korshunov.[11]

III. ANALYTICAL RESULTS

A convenient theoretical framework for the discussion of the phase diagram of the above model is the sine-Gordon field theory.[18] This theory yields a systematic expansion of the Green function $G(k,\omega)$, describing the effective interaction between two charges, including all the screening effects of the other charges. The expansion parameter is the activity y_0, which controls the fluctuations of the charges. This approach was followed in both Refs. 11 and 12. In Fig. 2 we display the phase diagram found in Ref. 11. The action for the creation of one pair of charges with opposite sign with unit separation in the time direction defines the activity

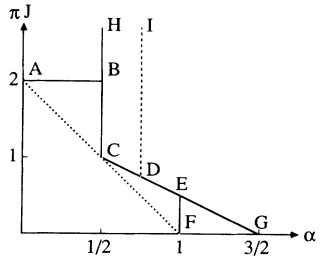

FIG. 2. Phase diagram of the same system as in Fig. 1 as obtained in Ref. 11.

$$y_0=\exp\{2\pi^2[G_0(j=0,\tau=1)-G_0(j=0,\tau=0)]\}\ . \tag{10}$$

Here and in the following we have scaled τ in units of $1/\sqrt{8E_JE_C}$. The effective Green function $G(k,\omega)$ is related to the bare $G_0(k,\omega)$ by Dyson's equation

$$G^{-1}(k,\omega)=G_0^{-1}(k,\omega)-\Sigma(k,\omega)\ . \tag{11}$$

The self-consistent contribution to the self-energy to first order in y_0 is

$$\Sigma_1=-8\pi^2y_0\exp[-2\pi^2G(j=0,\tau=0)]\ . \tag{12}$$

This contribution allows us already to find a rough division between ordered and disordered phases. From Eqs. (11) and (12) we find a transition line (line AF in Fig. 2)

$$\pi J=2-2\alpha\ . \tag{13}$$

Above this line in a J-α plot, Σ_1 vanishes, which implies order, and below Σ_1 has a finite value, implying disorder.[12] Additional features show up if the self-energy is evaluated self-consistently to second order in the activity:[11]

$$\Sigma_2(k,\omega)=-8\pi^2y_0^2\sum_{j,\tau}[1-\cos(kj+\omega\tau)]\exp\{4\pi^2[G(j,\tau)-G(j=0,\tau=0)]\}\ . \tag{14}$$

In analogy to G_0 in Eq. (9), we split the effective interaction G and similarly $\Sigma_2(k,\omega)$ into an isotropic and an anisotropic part. Hence,

$$\Sigma_2(k,\omega)=\Sigma_2^I+\Sigma_2^A+\Sigma_2^{A'}\ , \tag{15}$$

with

$$\Sigma_2^I(k,\omega)=-8\pi^2\tilde{y}_0^2\sum_{j,\tau}[1-\cos(kj+\omega\tau)]\exp\{4\pi^2[G^I(j,\tau)-G^I(j=0,\tau=0)]\}\ ,$$

$$\Sigma_2^A(\omega)=-8\pi^2 y_0^2 \sum_\tau [1-\cos(\omega\tau)]\exp\{4\pi^2[G(j=0,\tau)-G(j=0,\tau=0)]\}\ , \tag{16}$$

$$\Sigma_2^{A'}(\omega)=8\pi^2 \tilde{y}_0^2 \sum_\tau [1-\cos(\omega\tau)]\exp\{4\pi^2[G^I(j=0,\tau)-G^I(j=0,\tau=0)]\}\ .$$

We introduced a new "effective" activity $\tilde{y}_0$ by

$$\tilde{y}_0=y_0\exp[-2\pi^2 G^A(j=0,\tau=0)]\ . \tag{17}$$

For $\alpha>\frac{1}{2}$ and large J, we will see below that $G^A(j=0,\tau=0)$ is infinite, so that $\tilde{y}_0$ vanishes. Then the only contribution to Σ_2 is Σ_2^A, which in leading order in ω becomes

$$\Sigma_2^A(\omega)=-8\pi^2 y_0^2\omega^2\int_1^\infty d\tau\,\tau^2\exp\{4\pi^2[G(j=0,\tau)-G(j=0,\tau=0)]\}\ . \tag{18}$$

If we replace in this expression G by G_0, it diverges at the line $\pi J=\frac{3}{2}-\alpha$ (line *CDEG* in Fig. 2). Analogously to the KTB transition,[19] however, one finds by renormalization-group procedures that the phase transition takes place slightly above this line.[11]

For large J and $\alpha>\frac{1}{2}$, Korshunov[11] evaluated also a fourth-order contribution to the self-energy:

$$\Sigma_4(k,\omega)\propto -y_0^4 k^2|\omega|^\gamma\ , \tag{19}$$

with $\gamma=2$ for $\alpha>\frac{3}{4}$ and $\gamma=4\alpha-1$ for $\alpha<\frac{3}{4}$. This is line *ID* in Fig. 2. A self-energy of this form can only exist self-consistently if $\alpha>\frac{1}{2}$,[11] hence indicating that a phase transition will occur at $\alpha=\frac{1}{2}$.

Below the transition line $\pi J=\frac{3}{2}-\alpha+O(y_0^2)$, the isotropic interaction is screened, and for $\alpha>1$ we write Σ_2^A as

$$\Sigma_2^A(\omega)=-16\pi^2 y_0^2|\omega|^{2\alpha-1}\int_{|\omega|}^\infty dx(1-\cos x)x^{2\alpha}\ , \tag{20}$$

with $x=|\omega\tau|$. The integral in Eq. (20) converges in the limit $\omega\to 0$, and so $\Sigma_2^A(\omega)\propto -y_0^2|\omega|^\gamma$ for small ω, with $\gamma=2\alpha-1$. Evaluating G by Eq. (11), one indeed finds that the isotropic part of the interaction G^I is screened by a self-energy of this form. One can further check that in this region the first-order contribution Σ_1, given by Eq. (12), vanishes. If α becomes smaller than 1, however, one self-consistently finds a finite Σ_1, which screens both isotropic and anisotropic parts of the interaction. This is the transition line *DE* in Fig. 2.

Of course, the above only applies if $G^A(j=0,\tau=0)$ is self-consistently found to be infinite, which is the case for $\alpha>\frac{1}{2}$ and large J, as we will show now. If it is finite, meaning that the anisotropic part of the interaction is screened, the contributions Σ_2^I and $\Sigma_2^{A'}$ in Eq. (15) come into play. Now the contribution Σ_2^I is the dominant one because when G_0 is inserted into Eqs. (16) this contribution diverges at $\pi J=2$, whereas the anisotropic contributions diverge only at $\pi J=\frac{3}{2}$. To leading order in k and ω, we can write $\Sigma_2^I=-(c_1k^2+c_2\omega^2)$, with constants $c_1,c_2>0$, which depend on the exact location in the phase diagram and need not to be specified here. However, a term $-c_1k^2$ in the self-energy will screen the anisotropic part of the interaction. For $G^A(j=0,\tau=0)$ we now find, from Eq. (11),

$$G^A(j=0,\tau=0)=-\frac{\alpha}{2\pi^2}\ln(2\alpha c_1)\ . \tag{21}$$

Together with Eqs. (17) and (21), we then find

$$\tilde{y}_0\propto y_0^{1/(1-2\alpha)}\quad\text{for }\alpha<\tfrac{1}{2}\ , \tag{22}$$

independent of J, whereas $\tilde{y}_0$ vanishes for $\alpha>\frac{1}{2}$. This transition (line *HBC* in Fig. 2) occurs for large values of J, where the first-order contribution to the self-energy Σ_1 vanishes.

For $\alpha<\frac{1}{2}$ Korshunov[11] concluded that the Coulomb gas is equivalent to an isotropic Coulomb gas with activity $\tilde{y}_0$. Consequently, he predicted a KTB transition to occur at $\pi J=2$ in the limit of vanishing activity, independent of α (line *AB* in Fig. 2).

Korshunov[11] also included in his model a mutual capacitance between the grains. The main effect of this is a reduction of the activity of the charges; the large-distance behavior of the interactions, which determines the critical properties, is unchanged.

The interpretation of the phase transitions found above is the following. For $\alpha<\frac{1}{2}$ the situation is qualitatively the same as in the isotropic Coulomb gas. For large J we have a dielectric phase where the charges are ordered in dipoles. For small J we have a disordered or plasma phase where the charges are free. In the dipole phase we have *global* order in the phases, but no *local* order: The phase difference across the junctions is delocalized in time. At $\alpha=\frac{1}{2}$ and large J, we have a transition from a dipole to a *quadrupole* phase.[12] The origin of this transition is the anisotropic interaction: Considering two dipoles with the same space coordinates but with separation in time large compared to the sizes of the dipoles, we see that the isotropic part of their interaction is screened, but the anisotropic logarithmic interaction is doubled and gets a prefactor 4α. Consequently, a binding of dipoles into quadrupoles occurs at $\alpha=\frac{1}{2}$. In the quadrupole phase we have global as well as local order. For $\frac{1}{2}<\alpha<1$, if J is decreased, the quadrupoles unbind directly into free charges. For $\alpha>1$ with decreasing J, the quadrupoles unbind into dipoles oriented in the τ direction, a phase in which the isotropic interaction is screened, and the junctions behave independently. In this phase global order is destroyed, but we still have local or-

der. Of course, it has to be realized that the use of the Villian transformation casts doubt on the results obtained for too small J.

IV. MONTE CARLO RESULTS

In order to check the various predictions of the theory, we performed a Monte Carlo simulation for a Coulomb gas with interaction given by Eq. (8). Periodic boundary conditions in space and time were assumed (implying an Ewald summation), and so the system actually corresponds to a ring-shaped chain. The size of the system in the time direction is proportional to the inverse temperature of the model. In our program we employed many of the ideas of Saito and Müller-Krumbhaar,[20] who performed a Monte Carlo simulation on the isotropic 2D Coulomb gas. In particular, we used an enhanced rate of creation and annihilation of charges, as compared to the Metropolis rate, to speed up the simulation. The diffusion of charges was performed according to the Metropolis prescription. However, there exists an important difference to the isotropic case, namely, the charge creation and annihilation and charge diffusion have to be consistent with the neutrality condition in time at each junction. The different processes of creation-annihilation and diffusion which we allowed in our simulations are depicted schematically in Fig. 3. In one cycle of the program, each of these processes is attempted consecutively. Every 1000 cycles the charge configuration is recorded, from which we calculate the charge-charge correlation function $\langle p(j,\tau)p(j',\tau')\rangle$, the most important quantity extracted from the simulations.

As in the isotropic case, the KTB transition for small α manifests itself in the behavior of the dielectric constant. For large J the Coulomb gas is in a dipole phase, with finite constant, whereas for small J we have a disordered phase, with infinite dielectric constant. The dielectric constant at finite wave vector and frequency $\epsilon(k,\omega)$ is related to the charge-charge correlation function by

$$\epsilon^{-1}(k,\omega)=1-4\pi^2 G_0(k,\omega)\langle |p(k,\omega)|^2\rangle/N \ . \qquad (23)$$

In Fig. 4 we display results for the inverse dielectric constant $\epsilon^{-1}(k=0,\omega)$ of our Coulomb gas at $\alpha=0$, for

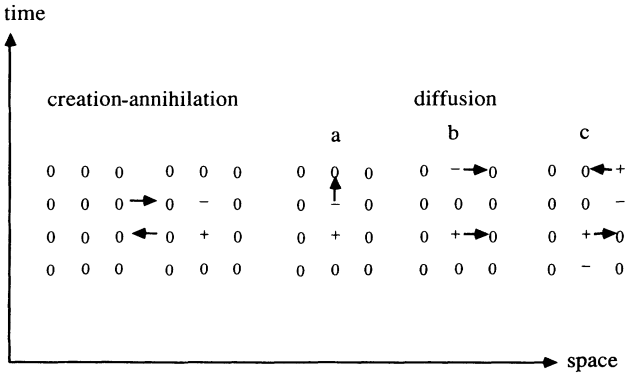

FIG. 3. Different processes of creation and annihilation and diffusion used in the program. Each of these processes is attempted once during a cycle.

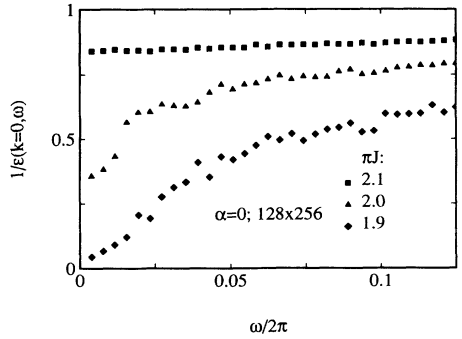

FIG. 4. Inverse dielectric constant vs frequency ω at $k=0$ and $\alpha=0$ for a 128×256 system in space-time, averaged over 2000 configurations. The KTB transition occurs between $\pi J=1.9$ and 2.0.

different values of J and for a system size of 128×256 in space-time (a system size of $2^n\times2^m$ allows use of the simplest fast-Fourier-transform algorithm). The estimated decorrelation time for the simulation with $\pi J=2$ and $\alpha=0$ was a few thousand cycles. The scatter of the data is a reliable measure of the statistical uncertainty. The behavior of ϵ^{-1} is comparable to that found in Ref. 20. At the transition, dipoles unbind into free charges. This occurs at a value of πJ between 1.9 and 2.0, which is about 20% lower than the transition found for the isotropic case [$\pi J\approx2.32$ (Ref. 20)]. The reason for this difference is the charge neutrality condition at each junction, which restricts the allowed configurations considerably, even in a large system, and favors the ordered state. In the neighborhood of the transition, the density of charges is very low, $\pm1\%$, and so the condition that a charge on a junction should have a partner with opposite sign on the same junction is quite stringent (this is the reason why we choose the size in the time direction preferably larger than that in the space direction). Indeed, the transition was observed to shift upward with increasing size in the time direction. However, we could not perform a reliable finite-size analysis of this effect.

For finite α but still small, $0<\alpha<\frac{1}{2}$, the transition is found to have qualitatively the same character, but it shifts to lower J.

The formation of quadrupoles should be signaled by a change in the charge-charge correlation function $\langle p(j,\tau)p(j,\tau')\rangle$ in time at a particular junction j. In Fig. 5 we plot, again for the 128×256 system, for $\pi J=1.5$ and different α, the function

$$S(\omega)\equiv\frac{\langle |p(j,\omega)|^2\rangle}{2\pi N_\tau|\omega|} \ . \qquad (24)$$

In the limit $\omega\to0$ this quantity can be interpreted as a "local resistance" of one junction (see the next section). A clear transition is seen at a value of α, which appears to be exactly $\frac{1}{2}$, in agreement with the analytical prediction.

For $\frac{1}{2}<\alpha<1$ the transition to the disordered phase when J is decreased changes character. It is now a transition from a quadrupole phase to a phase with free

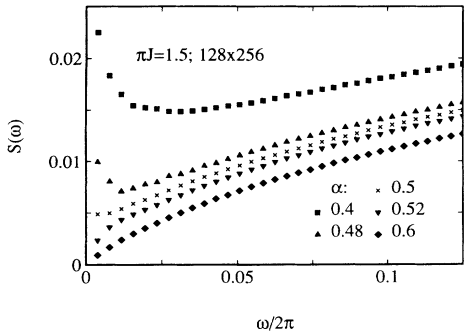

FIG. 5. Function $S(\omega)$ [Eq. (26)] at $\pi J=1.5$ for a 128×256 system, averaged over 4000 configurations. In the limit $\omega\rightarrow0$, this function can be interpreted as a "local resistance." The phase transition from a dipole phase to a quadrupole phase occurs at $\alpha=\frac{1}{2}$.

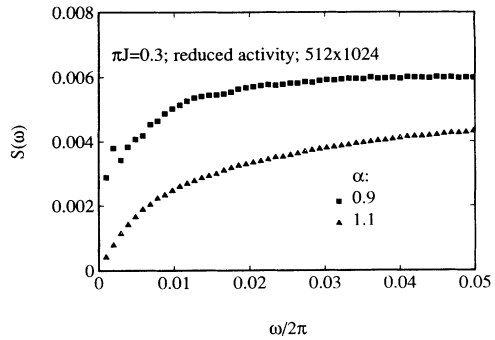

FIG. 6. Function $S(\omega)$ at $\pi J=0.3$ and 400 times reduced activity for a 256×1024 lattice. Average over 5600 configurations. The phase transition from a disordered phase to a phase with only local order occurs at $\alpha=1$.

charges. This transition can be found either by monitoring the function $S(\omega)$ [Eq. (24)] or the dielectric constant [Eq. (23)]. The location of the transition is now virtually independent of the size in the time direction. When moving to larger α, we could gradually decrease the size in the space direction from 128 to 16—keeping the size in time direction 256—in order to avoid exceedingly long simulation times (the charge density increases exponentially with decreasing J).

Beyond $\alpha=1$ the transition should again change character according to the analytical predictions. We do not clearly see this change in character (see also below), but can still follow the location of the transition line as a function of J. As it stands, we are not able to resolve with our simulation a clear transition from the disordered phase to a phase with only local order as a function of α at $\alpha=1$ and small J. The reason for this is the extremely high charge density in this region. However, according to the theoretical prediction, the transition should be independent of the activity y_0. Hence we artificially decreased the activity y_0, hoping that the location of the transition is unaltered. Physically, this corresponds to including in the model a mutual capacitance between the islands.[11] In Fig. 6 we display results for the function $S(\omega)$ of simulations for a 256×1024 system with a 400 times reduced activity, showing that a transition occurs between $\alpha=0.9$ and 1.1.

The phase diagram resulting from our simulations is depicted in Fig. 1. For $\alpha>\frac{1}{2}$ the theoretical transition line following from the scaling relations (19) lies slightly above the transition line found from the simulations. According to Korshunov,[11] the KTB transition should occur at $\pi J=2$ for $\alpha\leq\frac{1}{2}$ and at $\pi J=1+O(y_0^2)$ for $\alpha\geq\frac{1}{2}$ with a discontinuity at $\alpha=\frac{1}{2}$. In our simulations we do not see any indication for a vertical part at $\alpha=\frac{1}{2}$ of the transition between quadrupole and disordered phase, although we have checked this for different system sizes.

We have to stress that Fig. 1 is not the phase diagram of the original model [Eq. (1)], because of the use of the approximate Villain transformation, valid only for $E_J\gtrsim8E_C$. In the actual model, the horizontal transitions will be shifted (upward, because the Villain transformation overestimates the actual Josephson potential). In particular, we cannot exclude the possibility that the phase with only local order extends to $\alpha=\infty$. The vertical transitions, however, result from the dissipative interaction, which is taken into account exactly. It is reassuring that the transition at $\alpha=1$ matches the one found in the small-J limit.[8,12] We further mention that phase diagrams similar to Fig. 1 were found in 2D and 3D dissipative arrays of Josephson junctions.[9]

We also investigated the various theoretical predictions for the self-energy in the different regions of the phase diagram. The self-energy is related to the charge-charge correlation function by

$$\Sigma(k,\omega)=\frac{-4\pi^2\langle|p(k,\omega)|^2\rangle/N}{1-4\pi^2G_0(k,\omega)\langle|p(k,\omega)|^2\rangle/N}\ . \tag{25}$$

In Fig. 7 we plot results for Σ in the three different ordered regions. In the dipole phase we indeed find a self-energy of the form $-(c_1k^2+c_2\omega^2)$ for small k and ω, where c_1 and c_2 are positive constants depending on the

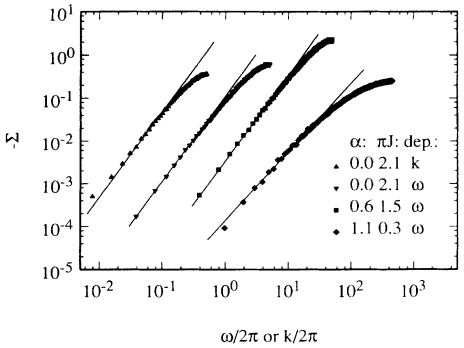

FIG. 7. Self-energy following from simulations in the three different ordered regions of the phase diagram. For the result in the dipole region ($\alpha=0$, $\pi J=2.1$), we plot both ω and k dependence: $\Sigma(k=0,\omega)$ and $\Sigma(k,\omega=2\pi/N_\tau)$ (we cannot put $\omega=0$ because of the pole in the interaction at $\omega=0$). For the results in the quadrupole region, we plot only $\Sigma(k=0,\omega)$. In the dipole and quadrupole phases, the results agree with a quadratic dependence. For the simulation in the phase with only local order ($\alpha=1.1$, $\pi J=0.3$), we find a power-law dependence $|\omega|^\gamma$, with $\gamma\approx1.6$. For clarity we shifted each data set one decade to the right of the previous one.

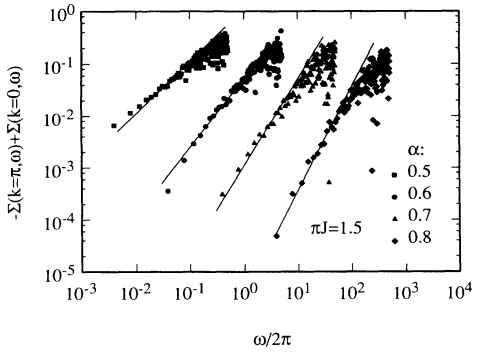

FIG. 8. Difference between the self-energy $\Sigma(k=0,\omega)$ and $\Sigma(k=\pi,\omega)$ in the quadrupole phase. The results are consistent with a power-law dependence $|\omega|^{\gamma}$, with $\gamma=4\alpha-1$ for $\frac{1}{2}<\alpha<\frac{3}{4}$ and $\gamma=2$ for $\alpha>\frac{3}{4}$ (drawn lines). For clarity we shifted each data set one decade to the right of the previous one.

precise values of J and α. On approaching the line $\alpha=\frac{1}{2}$, c_1 decreases and vanishes at $\alpha=\frac{1}{2}$. In the quadrupole phase, the self-energy is of the form $-c\omega^2$ for $k=0$. In the phase with only local order, we find, for the simulation performed at $\pi J=0.3$, $\alpha=1.1$ and for reduced activity, a self-energy of the form $-c|\omega|^{\gamma}$ at $k=0$ with $\gamma\approx 1.6$, whereas the theoretical prediction is $\gamma=1.2$. The reason for the difference remains unclear, but the exponent is definitely smaller than 2, which means that we are dealing with a different phase. In order to investigate the prediction (19) for the contribution to the self-energy of fourth order in y_0, we calculated the self-energy at $k=\pi$ in the quadrupole phase for different values of α. We subtracted from this the self-energy at $k=0$, thereby revealing the tiny y_0^4 contribution. The results are plotted in Fig. 8. Within the rather large error, this contribution indeed has an ω dependence in agreement with Eq. (19).

Concluding this section, we can say that we have proven by our Monte Carlo simulations the existence of the four phases which were predicted analytically. However, we find differences in the locations of the phase boundaries, the most important being the absence of a vertical part in the transition line between dipole (I) and disordered (II) phases, which was predicted by Korshunov.[11] On the other hand, his analytic expressions for the self-energy in the different phases turn out to be quite accurate.

V. RESPONSE FUNCTIONS

In Sec. III we reviewed the analytical predictions for the phase diagram and behavior of the self-energy in the different parts of the phase diagram. In Sec. IV we verified these predictions by Monte Carlo simulations. The self-energy and charge-charge correlation are related by Eq. (25), which, when inverted, reads

$$\langle |p(k,\omega)|^2\rangle=-\frac{N}{4\pi^2}\frac{\Sigma(k,\omega)}{1-G_0(k,\omega)\Sigma(k,\omega)} . \tag{26}$$

From (26) we can calculate every two-point correlation function of the system, in particular the correlation functions governing the linear response to an applied voltage, magnetic field, or current.

We will consider two experimental configurations to measure the transport properties. The first one is a ring-shaped chain of circumference N_x (assumed to approach infinity) to which we apply a flux $\Phi(t)$. This is equivalent to applying a voltage $V=\dot{\Phi}$. We will calculate the current in linear response and, from that, the conductance of the system. The second configuration is an infinite chain, with a current $I(t)$ imposed to flow through an open finite section of length L_x. We will calculate the voltage across this finite section and derive from that an expression for the impedance.

Before turning to the response functions in the different phases, it is instructive to consider the low-frequency impedance of a classical chain with either the Josephson channel present or absent. If the Josephson channel is absent, we simply have an RC chain with $R=R_S$. If the Josephson channel is present, we have, for low enough frequencies $\Omega L \ll R_S$, an LC chain with $L=1/4e^2E_J$. (For clarity we used Ω for the real frequency, to be distinguished from the imaginary and reduced frequency ω). The impedance Z of an infinite Z_0C chain where Z_0 can be either R_S or $i\Omega L$ (see Fig. 9) can be calculated by the recursion relation

$$Z=Z_0+\frac{1}{i\Omega C+1/Z} , \tag{27}$$

from which we find

$$Z=\frac{1}{2}Z_0\left[1+\left[1-\frac{4i}{Z_0\Omega C}\right]^{1/2}\right] . \tag{28}$$

For low frequencies we have

$$Z=\begin{cases}\sqrt{-iR/\Omega C} & \text{for } Z_0=R\\ \sqrt{L/C} & \text{for } Z_0=i\Omega L\end{cases} . \tag{29}$$

We now discuss the two configurations.

A. Configuration 1

The effect of a time-dependent flux $\Phi(t)$ enclosed by a circular chain of circumference N_x can be included by changing the boundary condition to $\varphi_{i=0}(\tau)=\varphi_{i=N_x}(\tau)-\Phi(\tau)$. Equivalently, we can shift the phases of the islands by

$$\varphi_n(\tau)\rightarrow\varphi_n(\tau)-n2e\frac{\Phi(\tau)}{N_x} , \tag{30}$$

where the index n now runs from $-\frac{1}{2}(N_x-1)$ to $\frac{1}{2}(N_x-1)$ (N_x is assumed to be odd). We note that the shift [Eq. (30)] with a time-dependent $\Phi(\tau)$ breaks the translational symmetry of the action due to the kinetic

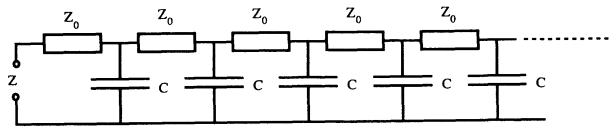

FIG. 9. Infinite Z_0C chain.

term. The equilibrium current $I(\tau)$ through the system can now be obtained from the thermodynamical relation

$$I(\tau)=\frac{\delta \ln Z}{\delta \Phi(\tau)} . \tag{31}$$

Combining Eqs. (30) and (31), the action (1), and the Villain transformation, we obtain, in linear response,

$$I(\omega)=K(\omega)\Phi(\omega) , \tag{32}$$

with a kernel $K(\omega)$ given by

$$K(\omega)=-\frac{4e^2E_J}{N_x}\left[1+\lambda|\omega|-4\pi^2\frac{J}{N}\langle|p(k=0,\omega)|^2\rangle/\omega^2 + \frac{\omega^2}{N_x}\sum_n n^2 - \frac{J}{N}\omega^4\sum_{n,n'} nn'\langle\varphi_n(\omega)\varphi_{n'}(-\omega)\rangle\right] , \tag{33}$$

in which we have also used Eq. (6). In the limit $\omega\to 0$ the kernel $K(\omega)$ defines a superfluid density n_s. We also obtain the conductance $\sigma(\Omega)$ from it after analytic continuation to real frequencies (and also undoing the rescaling of ω):

$$\sigma(\Omega)=\frac{1}{i\Omega}K(\omega\to -i\Omega/\sqrt{8E_JE_C}) . \tag{34}$$

If $\omega\ll 1/N_x$, the last two terms in Eq. (33), which result from the shift (30) in the kinetic term of the action, can be neglected. Using the definition (23) of the dielectric constant, we see that the first and third term between the square brackets in Eq. (33) combine to give the inverse dielectric constant $\epsilon^{-1}(k=0,\omega)$. From Eq. (26) and the form of the self-energy in the different phases, we can now evaluate the kernel $K(\omega)$ in the limit $\omega\to 0$. In phases (II) and (III), we have a finite dielectric constant, which was confirmed by the Monte Carlo simulations. Consequently, we find a finite superfluid density in these phases. With $\Sigma=-(c_1k^2+c_2\omega^2)$ in phase (II), $\Sigma=-(c_1k^2|\omega|^\gamma+c_2\omega^2)$ in phase (IIIa), and $\Sigma=-c\omega^2$ in phase (IIIb), we obtain superfluid densities $n_s=4e^2E_J/(1+Jc_2)$, $4e^2E_J/(1+Jc_2)$, and $4e^2E_J/(1+Jc)$ in these phases, respectively. Evaluating the conductance by Eq. (34), we find $\sigma=1/N_xR_S$ for $\Omega\to 0$ in phase (I) and infinite conductance in phases (II)–(IV). The striking result here is that we find no finite superfluid density in phase (IV), but we do find an infinite conductance.

If $\omega\gg 1/N_x$, the last two terms in Eq. (33) are the dominant ones. They can be evaluated further by using the Fourier transform $n(k)$ of the function n:

$$n(k)=\begin{cases}0 & \text{for } k=0\\ \dfrac{N_x}{ik}(-1)^{N_xk/2\pi} & \text{otherwise .}\end{cases} \tag{35}$$

These terms can then be rewritten as

$$N_x\omega^2\int_{-\pi}^{\pi}\frac{dk}{2\pi}\frac{1}{k^2}\left[1-\frac{J}{N}\omega^2\langle|\varphi(k,\omega)|^2\rangle\right] , \tag{36}$$

where we replaced the sum over k by an integral. The phase-phase correlation function can be expressed in terms of the charge-charge correlation function by means of Eqs. (4) and (6):

$$\langle|\varphi(k,\omega)|^2\rangle=\frac{N}{J}\frac{1}{\omega^2+\lambda|\omega|k^2+k^2} + 4\pi^2\frac{k^2/\omega^2}{(\omega^2+\lambda|\omega|k^2+k^2)^2}\langle|p(k,\omega)|^2\rangle . \tag{37}$$

The first term in this expression is the spin-wave contribution. We now see that the apparently divergent integral in Eq. (36) is actually convergent. With the help of Eq. (26) and the expressions for the self-energy found in the different phases, we can now evaluate expression (36). We note that when $\omega\ll 1$ (but still $\omega\gg 1/N_x$), the integrand in (36) decays at least $\propto 1/k^2$, so that we may replace the integration boundaries by $\pm\infty$. We can then use the method of contour integration. It is now only a technical matter to determine the poles in the different regions of the phase diagram and to evaluate their residues. After applying Eq. (34) to the kernel $K(\omega)$, we find, for the conductance $\sigma(\Omega)$ in the different phases to leading order in Ω,

$$\text{(I)}\quad \Sigma(k,\omega)=-c\to\sigma(\Omega)=\tfrac{1}{2}(i\Omega C/R_S)^{1/2} ,$$

$$\text{(II)}\quad \Sigma(k,\omega)=-(c_1k^2+c_2\omega^2)\to\sigma(\Omega)=\tfrac{1}{2}[4e^2E_JC/(1+Jc_1)(1+Jc_2)]^{1/2} ,$$

$$\text{(IIIa)}\quad \Sigma(k,\omega)=-(c_1k^2|\omega|^\gamma+c_2\omega^2)\to\sigma(\Omega)=\tfrac{1}{2}[4e^2E_JC/(1+Jc_2)]^{1/2} , \tag{38}$$

$$\text{(IIIb)}\quad \Sigma(k,\omega)=-c\omega^2\to\sigma(\Omega)=\tfrac{1}{2}[4e^2E_JC/(1+Jc)]^{1/2} ,$$

$$\text{(IV)}\quad \Sigma(k,\omega)=-c|\omega|^\gamma\to\sigma(\Omega)=-2e^2E_J(Jc)^{-1/2}(-i\Omega/\sqrt{8E_JE_C}\omega)^{2-\gamma/2} .$$

Here c, c_1, and c_2 are positive constants depending on the precise position in the phase diagram. We see that in the disordered phase (I) the response is that of an RC chain with $R=R_S$ and that in the dipole (II) and quadrupole (III) phases the response is that of an LC chain with $L=\delta/4e^2E_J$ and δ (≥ 1) a constant which can be read off from Eqs. (38). In comparison with the result (29), there is a difference of a factor of 2. This is because in Eqs. (29) the impedance to ground is determined, whereas Eqs. (38) refer to the conductance measured between the first and last islands of the chain. In the phase with only local order (IV), we find an anomalous response, which is neither that of an RC nor that of an LC chain. We list these results in Table I.

B. Configuration 2

The second configuration is a very long chain, with a current $I(t)$ imposed to flow through a finite section of

length L_x, by connecting island $i=0$ to a current source and extracting the current at island $i=L_x$. The average voltage between islands $i=0$ and L_x defines a "local impedance" Z_{L_x}. The current I adds a term $I(\varphi_L-\varphi_0)/2e$ to the Hamiltonian of the system, and the voltage operator is defined by $V=\dot{\varphi}/2e$. Straightforward application of linear response yields

$$Z_{L_x}(\Omega)=\lim_{I\to 0}\langle V_{L_x}-V_0\rangle/I=\frac{R_Q}{2\pi}i\Omega D(\Omega+i0^+)\ , \quad (39)$$

where $D(\Omega)$ is the time Fourier transform of the retarded correlation function of the phase difference between islands 0 and L_x:

$$iD(t-t')=\Theta(t-t')\langle[\varphi_{L_x}(t)-\varphi_0(t),\varphi_{L_x}(t')-\varphi_0(t')]\rangle\ . \quad (40)$$

We evaluate this correlation function in imaginary time and then perform the analytical continuation to real time. We then find

$$Z_{L_x}(\Omega)=\left[\frac{R_Q}{2\pi N_\tau}|\omega|\langle|\varphi_{i=L_x}(\omega)-\varphi_{i=0}(\omega)|^2\rangle\right]$$
$$=\left[\frac{R_Q}{2\pi N_\tau}|\omega|\frac{1}{N_x}\int_{-\pi}^{\pi}\frac{dk}{2\pi}2[1-\cos(kL_x)]\langle|\varphi(k,\omega)|^2\rangle\right]\ , \quad (41)$$

where $\omega\to -i\Omega/\sqrt{8E_JE_C}$, and we have replaced the summation over k by an integral.

If $1/L_x\ll\omega\ll 1$, we can again replace the integration boundaries in Eq. (41) by $\pm\infty$ and apply the method of contour integration. The contribution of the cosine in the integrand of Eq. (41) is negligible because of its rapid oscillations. We find exactly the same response as in configuration 1, except in the dipole phase (II), where instead of the response of an LC chain we find the response of an RC chain, but with a reduced resistance $R=[Jc_1/(1+Jc_1)]^{1/2}R_S$ for $\Sigma=-(c_1k^2+c_2\omega^2)$. This is a very peculiar result. We note, however, that $Jc_1\to 0$ if $J\to\infty$ (c_1 itself also depends on J), and so in this limit these results do not contradict each other.

In the other case $\omega\ll 1/L_x$, we use Eqs. (37), (26), and the expressions for the self-energy in the different phases. Remembering that k^2 was an abbreviation of $2(1-\cos k)$ and making use of the fact that

$$\int_{-\pi}^{\pi}\frac{dk}{2\pi}\frac{1-\cos(kL_x)}{1-\cos k}=L_x\ , \quad (42)$$

we find resistive behavior in the disordered phase (I) *and* in the dipole phase (II), with $Z=L_xR_S$. In phases (III) and (IV), we find zero resistance. We could try to derive an expression for the superfluid density in these phases, by inverting the impedance to get the conductance, then multiplying the conductance by $i\Omega$, i.e., the reverse of Eq. (34), and finally taking the limit $\Omega\to 0$. Following this procedure, we find a finite superfluid density *only* in phase (IIIb). We include these results also in Table I. We further note that, according to recent calculations of Panyukov and Zaikin,[13] the response of an open chain to an applied voltage yields, in the limit of small frequencies, a conductance which is the inverse of the resistance of an open chain with an applied current. This suggests that the difference in responses between configurations 1 and 2 arises because of the difference in the boundary conditions, which are "stronger" in configuration 1 than in configuration 2. In other words, if we fix the magnetic flux inside the ring (configuration 1), we do not allow for a certain type of quantum fluctuations of grain phases allowed for an open chain (configuration 2). As a result, the response functions for these two configurations differ in the phases (II) and (IIIa).

The main results of this paper are the phase diagram Fig. 1 and the response functions summarized in Table I. We have mapped out much of the interesting parameter range and obtained a rather complete phase diagram. There remain small uncertainties due to the finite-size effects inherent to our Monte Carlo simulations. The important differences with the analytical work of Korshunov[11] are the absence of a vertical part in the transition line between quadrupole (III) and disordered (I) phases and the finite slope of the transition line between dipole (II) and disordered (I) phases (compare Figs. 1 and 2).

The analysis of the response functions has yielded some surprises. The response may depend, even qualitatively, on the particular experiment performed. In particular, the dipole phase (II) shows a superconducting or a resistive response depending on the type of experiment. In the second configuration, where we determine the response to a current flowing through an open section of length L_x, the response functions for small and large frequencies $1/L_x\ll\omega\ll 1$ or $\omega\ll 1/L_x$ differ in phase (II). We recover apparently contradicting results obtained by Panyukov and Zaikin[9,13] or by Zwerger[10] in different setups or different limits. Panyukov and Zaikin considered the boundary conditions which correspond to a d-dimensional open system and calculated the response functions in the limit $\omega\ll k$ by means of an instanton technique. The results of their calculations and ours for a 1D open chain essentially coincide in the above-

mentioned limit. However, they did not consider the situation of an externally fixed magnetic flux in a ring geometry and hence did not discuss the superconducting properties (finite superfluid density) of the phase (II). On the other hand, Zwerger[10] missed the difference between the dipole phase (II) and the quadrupole phase (III). But these phases differ dramatically in several response properties.

ACKNOWLEDGMENTS

It is a pleasure to acknowledge stimulating discussions with S. V. Panyukov and G. T. Zimanyi. The hospitality of the Technical University Delft towards one of us (A.D.Z.) allowed us to discuss our differing points of view and to resolve the discrepancies. The research of one of us (P.A.B.) has been made possible by support from the Royal Netherlands Academy of Arts and Sciences.

---

*Permanent address: Istituto di Fisica, Facolta di Ingegneria, Università di Catania, Italy.

[1]B. G. Orr, H. M. Jaeger, A. M. Goldman, and C. G. Kuper, Phys. Rev. Lett. **56**, 378 (1986); H. M. Jaeger, D. B. Haviland, B. G. Orr, and A. M. Goldman, Phys. Rev. B **40**, 182 (1989).

[2]L. G. Geerligs and J. E. Mooij, Physica B **34**, 212 (1988); L. G. Geerligs *et al.*, Phys. Rev. Lett. **63**, 326 (1989).

[3]V. Ambegaokar, U. Eckern, and G. Schön, Phys. Rev. Lett. **48**, 1745 (1982); U. Eckern, V. Ambegaokar, and G. Schön, Phys. Rev. B **30**, 6419 (1984).

[4]A. O. Caldeira and A. J. Leggett, Ann. Phys. (N.Y.) **149**, 374 (1983).

[5]S. Chakravarty, G. L. Ingold, S. Kivelson, and A. Luther, Phys. Rev. Lett. **56**, 2303 (1986); A. Kampf and G. Schön, Phys. Rev. B **36**, 3651 (1987); M. P. A. Fischer, *ibid.* **36**, 1917 (1987); B. Mirhashem and R. A. Ferrell, Physica C **152**, 361 (1988); Phys. Rev. B **37**, 649 (1988).

[6]S. V. Panyukov and A. D. Zaikin, Phys. Lett. A **124**, 325 (1987); S. Chakravarty, S. Kivelson, G. T. Zimanyi, and B. I. Halperin, Phys. Rev. B **37**, 7256 (1988); A. Kampf and G. Schön, *ibid.* **37**, 5954 (1988); Physica B **152**, 239 (1988); W. Zwerger, J. Low Temp. Phys. **72**, 291 (1988).

[7]J. Choi and J. V. José, Phys. Rev. Lett. **62**, 1904 (1989); R. Fazio, G. Falci, and G. Giaquinta, Solid State Commun. **71**, 275 (1989).

[8]S. Chakravarty, G. L. Ingold, S. Kivelson, and G. T. Zimanyi, Phys. Rev. B **37**, 3283 (1988).

[9]A. D. Zaikin, Physica B **152**, 251 (1988); S. V. Panyukov and A. D. Zaikin, J. Low Temp. Phys. **75**, 361 (1989).

[10]W. Zwerger, Europhys. Lett. **9**, 421 (1989); W. Zwerger, Z. Phys. B **78**, 111 (1990).

[11]S. E. Korshunov, Europhys. Lett. **9**, 107 (1989); S. E. Korshunov, Zh. Eksp. Teor. Fiz. **95**, 1058 (1989).

[12]P. A. Bobbert, R. Fazio, G. Schön, and G. T. Zimanyi, Phys. Rev. B **41**, 4009 (1990).

[13]A. D. Zaikin, S. V. Panyukov, and A. D. Zaikin, Phys. Lett. A **156**, 119 (1991).

[14]R. Fazio and G. Schön, in *Transport Properties of Superconductors—Progress in High T_c*, edited by R. Nikolsky (World Scientific, Singapore, 1990), Vol. 25, p. 298; and Phys. Rev. B **43**, 5307 (1991).

[15]A. Schmid, Phys. Rev. Lett. **51**, 1506 (1983); S. A. Bulgadaev, Pis'ma Zh. Eksp. Teor. Fiz. **39**, 264 (1984) [JETP Lett. **39**, 315 (1984)]; F. Guinea, V. Hakim, and A. Muramatsu, Phys. Rev. Lett. **54**, 263 (1985).

[16]R. M. Bradley and S. Doniach, Phys. Rev. B **30**, 1138 (1984).

[17]G. Schön and A. D. Zaikin, Physica B **152**, 203 (1988).

[18]P. Minnhagen, Rev. Mod. Phys. **59**, 1001 (1987).

[19]J. V. José, L. P. Kadanoff, S. Kirkpatrick, and D. R. Nelson, Phys. Rev. B **16**, 1217 (1977).

[20]Y. Saito and H. Müller-Krumbhaar, Phys. Rev. B **23**, 308 (1981).